Nano-indentation Measurement for Young's modulusof the Human Tooth Enamel

B. W. Haung[1], J.-G. Tseng[2], M. Z. Wong[3], P. J. Chiu[3], and J. H. Kuang[3*]

[1]Department of Mechanical Engineering, Cheng Shiu University, Kaohsiung, Taiwan
[2]Bachelor Program of Medical Engineering, Cheng Shiu University, Kaohsiung, Taiwan
[3]Department of Mechanical and Electro-Mechanical Engineering, National Sun Yat-sen University, Kaohsiung,Taiwan
*E-mail: kuang@faculty.nsysu.edu.tw

Abstract: The feasibility of employing simple loading and continuous stiffness measurement methods on the Young's modulus of human tooth enamel is investigated in this work. Different peak loads, i.e. 20, 60, 120 and 180 mN, are both applied in the loading and unloading for the simple load and the continuous stiffness measurement methods. The difference between the mean values and the standard deviations of measured Yonung's modulus are compared and evaluated. The variation between measured Young's modulus and the peak loads are also studied and discussed. The measured results indicate that the continuous stiffness measurement method can provide more reliable measured results.

1. Introduction

Human tooth, composed by organic matter and minerals, is one of the hardest human tissues and the major function of human tooth is used to cut and chew food. Dental disease [1, 2] will cause serious digestion problems. Due to the special distribution on the material of tooth, the mechanical properties differences of outer enamel and the inner dentin, and the limitation of the geometric shape and size, it is difficult to make a standard test piece of tooth for the conventional tensile testing. The dimension for the indenter of the Nano-indentation system is at nanometer level [3]. It can easily measure the mechanical properties of any local area on the surface of the test piece. And more over, it is simple to operate and effortless to make standard specimen. The surface roughness of the specimen can be managed to the test specifications apparently while the thickness of the material only need tenth of the measuring depth. To measure the mechanical properties of material is a basic and important work. It often determines the engineering application of the material. The reliable mechanical properties of tooth can be accurately predicted the behavior and destruction of the material by numerical simulation. It can also provide the reference data for the materials in tooth replacement related research [4, 5].

The nano-indentation technique presses the diamond probe, with known geometry and material parameters, into the test material. The contact area is calculated by the indentation depth sensors indirectly under full load. Young's modulus is computed from the initial unloading slope in load-deformation curve diagram. The Continuous Stiffness Measurement (CSM) superimposes the tiny simple harmonic vibration during loading [6, 7]. And by a single loading-unloading measurement procedure, we can get multiple sets of data on the depth and Young's modulus.

This research is to measure the Young's modulus of tooth enamel for four groups of different ages by using CSM of the nano-indentation system, and in addition to compare with the Young's modulus obtained from the average indentation depth of ± 50 nm (nanometer) by Simple loading Measurement (SLM).

2. Theory of Nano-indentation System
2.1 Simple Loading Measurement

Sheddon indicated that by any smoothing function of a rotating body, the load and displacement curve relationship (Figure 1) of an indenter could be expressed by the exponential law (power law) [8]:
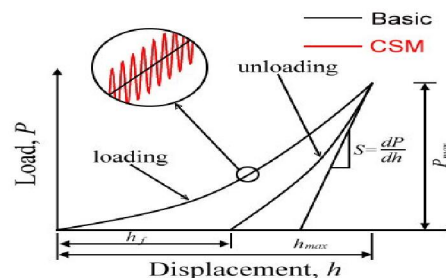

Figure 1. Load and displacement relationship concept diagram

$$P = \alpha(h - h_f)^m , \qquad (1)$$

where, α, m were constants and related to the geometry of the probe, h was the indentation depth, h_f was the residual indentation depth after unloading.

Oliver and Pharr [9] used Berkovich probe to the indentation tests for six different materials and found that all the load-displacement curves were nonlinear. But, it became linear in logarithmic coordinates and also indicated that the exponential relationship between load and displacement was correct [10]. It is supposed that the material experienced plastic deformation during loading process and elastic deformation in unloading period, the initial unloading slope in the load-displacement diagram could be defined as elastic contact stiffness (S) [11]:

$$S = \left.\frac{dP}{dh}\right|_{h_{max}} \qquad (2)$$

Indentation depth was the summation of probe contact depth (h_c) and contact displacement with the surrounding surface (h_s):

$$h = h_c + h_s \qquad (3)$$

It was also assumed that the contact portion between the material and the indenter was permanent plastic deformation and the outer surface area of the contact surface was elastic deformation. Then, h_s could be assumed only related to h_f:

$$h_s = \varepsilon(h - h_f) \qquad (4)$$

where, ε was the geometric correction factor. From (1) (2) (3) (4), one could get:

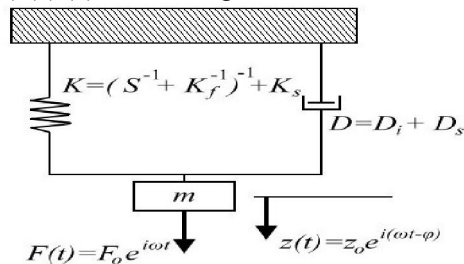
Figure 2   Equivalent dynamic model diagram of the nanoindentation measurement system

$$h_c = h - m\varepsilon\frac{P}{S} = h - \rho\frac{P}{S} \qquad (5)$$

and view $m\varepsilon$ as a new probe geometry factor ρ.

Oliver et al [12] used the iterative method to propose indentation area function: a perfect berkovich indentation contact area was:

$$A = 24.5h_c^2 \qquad (6)$$

The actual diamond probe was usually not in ideal condition and the surface area function would vary with the wear produced during operating period. Therefore, the contact area and contact depth

relationship was revised with the curve regression method:

$$A(h_c) = 24.5h_c^2 + \sum_{i=0}^{7} C_i h_c^{\frac{1}{2^i}} \qquad (7)$$

where, C_i was a constant and was defined by the experimental data of measuring the material with known mechanical properties via multiple different loading processes.

Sheddon assumed that the indentation probe was a perfect rigid body [8], i.e., the indenter did not deform any time during the contact process with the material.

The load and displacement relationship of the cylindrical indentation probe could be expressed as follows:

$$P = \frac{4Ga}{1-\nu}h \qquad (8)$$

where, G was the shear modulus of the specimen, ν was Poisson's ratio of the specimen, and a was the radius of the cylinder. By using the relationship between Young's modulus and shear modulus $E = 2G(1+\nu)$, the contact area of the cylinder $A = \pi a^2$, and the differentiation of indentation load with respect to indentation depth, one could get the following expression:

$$S = \frac{dP}{dh} = \frac{2}{\sqrt{\pi}}\sqrt{A}\frac{E}{1-\nu^2} \qquad (9)$$

Hence, the elastic modulus could be derived from the initial unloading slope. Because the actual measurement indenter was diamond, its elastic behavior needed to be considered. Tabor and Stillwell defined the reduce modulus, E_r, through experimental observation [13]:

$$\frac{1}{E_r} = \frac{(1-\nu^2)}{E} + \frac{(1-\nu_i^2)}{E_i} \qquad (10)$$

where, E_i and ν_i represent the Young's modulus and Poisson's ratio of the indentation probe, respectively. E and ν represent the Young's modulus and Poisson's ratio of the specimen, respectively. Using formula (10) to rewrite formula (9) as formula (11):

$$S = \frac{dp}{dh} = \frac{2}{\sqrt{\pi}}\sqrt{A}E_r \qquad (11)$$

Since formula (8) was used for cylindrical indenter, King obtained the geometry correction factor relationship of diamond indenter via finite element analysis as followed:

$$S = \frac{dp}{dh} = \beta\frac{2}{\sqrt{\pi}}\sqrt{A}E_r \qquad (12)$$

After obtaining indentation area indirectly through the depth sensor by formula (7), the reduce modulus, E_r, could be calculated by the initial unloading stiffness relationship (12). The Young's

modulus of the specimen could be calculated by formula (10) when it was substituted by the material parameters of diamond indentation probe and was estimated by the Poisson's ratio of the specimen.

2.1 Continuous Stiffness Measurement Technology

Oliver and Pharr took the lead in establishing the continuous stiffness measurement technology. In this way, one could not only continuously measure the mechanical properties of materials under different depths in the loading process but also draw the Young's modulus and the indentation depth relationship diagram.

Continuous stiffness measurement was to superimpose high-frequency and micro-vibration in the loading process (Figure 2). The load, $F(t)$, in the form of a simple harmonic motion was expressed as

$$F(t) = F_o e^{i\omega t} \qquad (13)$$

where, F_o was the amplitude of vibration load, ω was the angular frequency. It was assumed that the load $F(t)$ produced $Z(t)$ displacement onto the probe, the second-order vibration equation of motion of the entire system was:

$$m\ddot{z} + D\dot{z} + Kz = F(t) \qquad (14)$$

where, m was the mass of the probe, D was the effective damping coefficient of the entire system, i.e. the sum of the specimen damping D_s and the capacitive displacement damping D_i.

$$D = D_s + D_i \qquad (15)$$

The relationship of the effective stiffness K of the entire system was as followed:

$$K = (S^{-1} + K_f^{-1})^{-1} + K_s \qquad (16)$$

where, Ks was the stiffness of the support structure, K_f was the stiffness of the machine frame. The particular solution of equation (14) was:

$$z(t) = z_o e^{i(\omega t - \phi)} \qquad (17)$$

where, Z_o was the amplitude of vibration displacement, φ was the phase difference between the load and displacement signals and satisfied the following equation:

$$\tan\phi = \frac{\omega D}{K - m\omega^2} \qquad (18)$$

Differentiate equation (17) and substitute into equation (18), one could have:

$$\left|\frac{F_o}{z_o}\right| = \sqrt{(K - m\omega^2)^2 + (\omega D)^2} \qquad (19)$$

Rearrange (16) (18) (19) to get the stiffness S and contact damping ratio Ds:

$$S = \left[\frac{1}{\frac{F_o}{z_o}\cos\phi - (K_s - m\omega^2)} - \frac{1}{K_f}\right]^{-1} \qquad (20)$$

$$\omega D_s = \frac{F_o}{z_o}\sin\phi - \omega D_c \qquad (21)$$

Figure 3. Teeth specimens of different age

Young's modulus of the specimen could be easily obtained after substituting contact stiffness S calculated from equation (20) into equation (12).

3. Nano-indentation Test
3.1 Prototype of tooth specimen

The experiment that employs the 35-year-old, 46-year-old, 68-year-old and 75-year-old male molars as specimens is shown in Figure 3. It can be easily to determine the enamel and dentin on the cutting surface of the complete teeth by cleaning the teeth, fix them in epoxy resin, and grind 2 mm thickness of the tooth occlusal surface perpendicularly. The emery sandpapers of grain number from low to high (granulocyte No. 80, 800, 1200, and 2500) are used to gradually reduce the plane roughness. To burnish the surface of tooth, it is by using the fluff polishing cloth of the grinder with the polish slurries. . And then to remove the residual slurries and dry out the water on the surface of tooth by water rinsing. The theoretical surface roughness is 0.3 μm.

3.2 Nano-indenter Set Up

The nano-indentation system used in this experiment is Nano Indenter XP System, with Berkovich Erlenmeyer indentation probe, manufactured by MTS System Corporation, U.S.A., as shown in Figure 4. Two experiments are conducted, the basic load measurements and continuous stiffness measurement, to explore which is more appropriate for the measurement of biological materials by comparing these two sets of data.
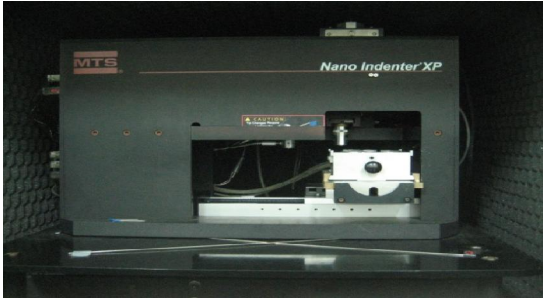
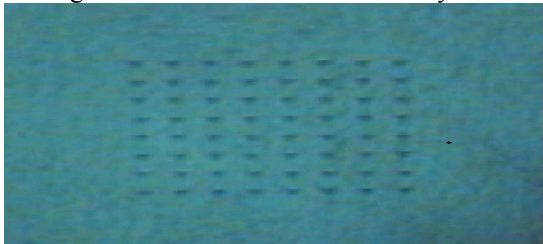Figure 4   MTS Nano Indenter XP system

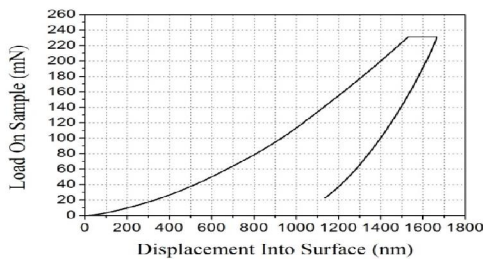Figure 5   Measuring dot matrix of the indentation test

Figure 6   Load and indentation depth diagram of CSM

By using the microscope lens of the measurement system to find out a relatively flat area of the tooth enamel and to set a 8×8 square matrix measurement points, the dots are separated by appropriate distance of 30 μm (more than seven times of the indentation depth), as shown in Figure 5. More than 50 points of data in each set are selected as the valid data. Set Poisson's ratio of the tooth enamel as 0.3. In CSM mode, set the
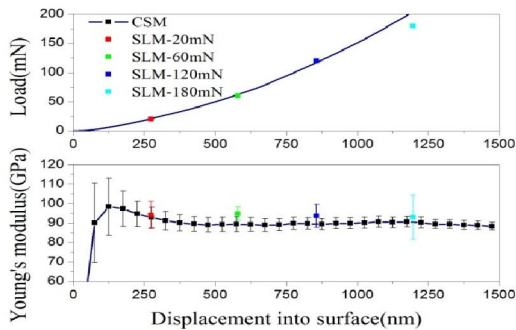

Figure 7. Load, Young's modulus, indentation depth diagram measured from 35 years old tooth.
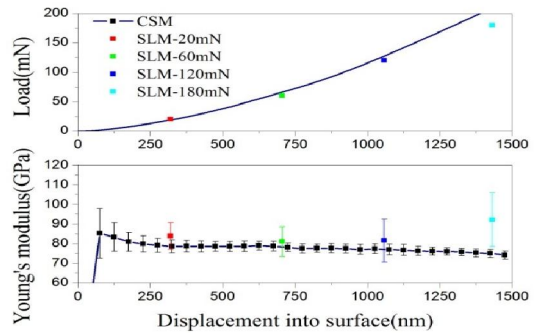

Figure 8. Load, Young's modulus, indentation depth diagram measured from 46 years old tooth.
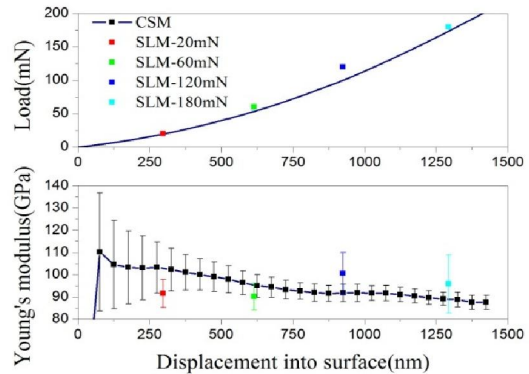

Figure 9. Load, Young's modulus, indentation depth diagram measured from 68-year-old tooth.

Following parameters: strain rate 0.05, vibration frequency 45 Hz, amplitude 2 nm, maximum measuring depth 1500 nm, allowable external disturbance (drift rate) 0.05 nm/s. Refer to CSM depth-loading diagram, SLM mode is setting as follows: peak loads as 20, 60, 120.
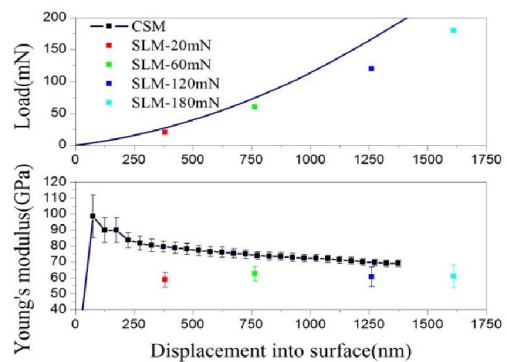

Figure 10   Load, Young's modulus, indentation depth diagram measured from 75-year-old tooth.

4. Experimental Results and Discussions

The relationship diagrams of load and Young's modulus with respect to indentation depth for different

Table 1. Difference of Young's moduli measured by SLM and CSM (35-year-old molars samples)

	SLM		CSM		
Max. loading (mN)	Indentation Depth (nm)	Young's modulus (GPa)	Standard Deviation	Young's modulus (GPa)	Standard Deviation
20	274	94.13	7.13	92.74	5.40
60	579	94.80	3.49	89.30	3.68
120	856	93.61	5.94	89.51	2.76
180	1196	92.93	11.34	90.46	2.56
Average		93.87		90.50	

Table 2   Difference of Young's moduli measured by SLM and CSM (46-year-old molars samples)

	SLM		CSM		
Max. loading (mN)	Indentation Depth (nm)	Young's modulus (GPa)	Standard Deviation	Young's modulus (GPa)	Standard Deviation
20	320	83.84	6.78	78.92	2.38
60	705	81.06	7.54	78.48	1.92
120	1058	81.59	10.93	77.25	2.32
180	1431	92.17	13.68	74.87	1.87
Average		84.67		77.38	

180 μN, loading and unloading rate 1 mN/s, load holding period 30 sec, allowable external disturbance (drift rate) 0.5 nm/s.

Table 3. Difference of Young's moduli measured by SLM and CSM (68-year-old molars samples)

	SLM		CSM		
Max. loading (mN)	Indentation Depth (nm)	Young's modulus (GPa)	Standard Deviation	Young's modulus (GPa)	Standard Deviation
20	297	91.59	6.34	103.87	6.82
60	614	90.14	6.08	95.72	3.65
120	924	100.48	9.42	91.77	3.29
180	1294	95.81	13.06	89.22	2.42
Average		94.50		95.15	

Table 4. Difference of Young's moduli measured by SLM and CSM (75-year-old molars samples)

SLM	CSM					
Max. loading (mN)	Indentation Depth (nm)	Depth	Young's modulus (GPa)	Standard Deviation	Young's modulus (GPa)	Standard Deviation
20	383		58.86	4.74	87.52	3.69
60	765		62.50	4.45	80.05	3.30
120	1261		60.65	6.22	74.04	3.82
180	1611		61.01	7.29		
Average			60.76		80.54	

Ages are shown in Figure 6 to 10. Young's moduli is obtained by SLM and CSM calculated with the average on the indentation depth of ±50 nm interval in the SLM is compared in Table 1 to 4, respectively. Where indentation depth measured less than 180 mN maximum load of SLM has exceeded CSM measurement range, as shown Table 4. Young's modulus distribution maps of tooth enamel of different ages are shown in Figure 11 to 16, where each column represents a 2 GPa interval range. In CSM mode, Young's modulus of the enamel decreases with increasing depth, similar to previous experimental results [14]. Current experiments show that the standard deviation of Young's modulus of the tooth enamel in higher depth of indentation area will gradually decrease and stabilize to a certain value in Gaussian distribution form, as shown in Figure 13 to 14.

The variations of Young's modulus and standard deviation are both large when the indentation depth is less than 400 nm, as shown in Figure 7 to 10. It is presumably because of greater influence by the surface roughness in low loading process and it increases the measurement error accordingly.
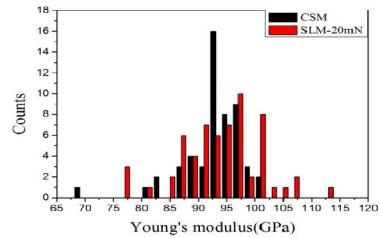

Figure 11 Young's modulus distribution maps of CSM and SLM with 20 mN max. load of 35 years old tooth.
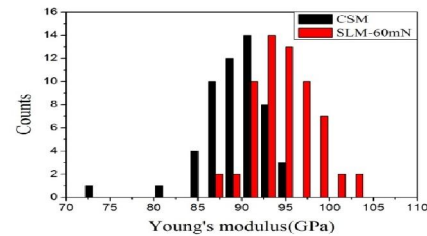

Figure 12 Young's modulus distribution maps of CSM and SLM with 60 mN max. load of 35-year-old tooth.
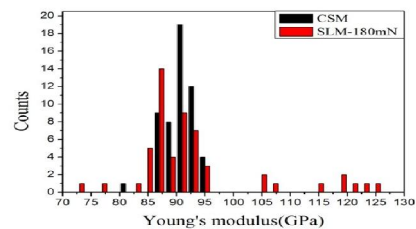

Figure 13 Young's modulus distribution maps of CSM and SLM with 180 mN max. load of 35-year-old tooth.

The Young's modulus measured by SLM does not decrease when the indentation depth increases in the experiments. It is a worth mentioning when the four sets of test pieces experiencing the maximum loading of 120 or 180 mN, standard deviation of Young's modulus will increase, while the Gaussian distribution is not obvious, and even twin peaks distribution will appear, as shown in Figure 14 and 15. When the maximum loading is 60 mN the pure Gaussian distribution appears, as shown in Figure 12 and 16.
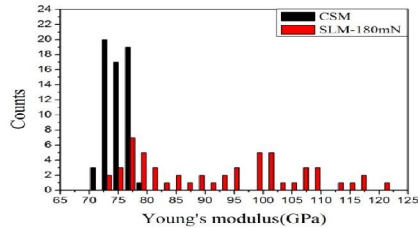

Figure 14 Young's modulus distribution maps of CSM and SLM with 180 mN max. load of 46-year-old tooth.
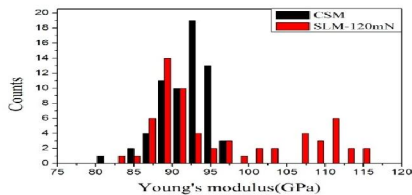

Figure 15 Young's modulus distribution maps of CSM and SLM with 120 mN max. load of 68-year-old tooth.
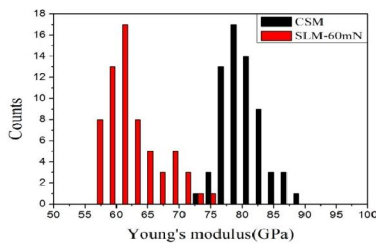

Figure 16 Young's modulus distribution maps of CSM and SLM with 60 mN max. load of 75-year-old tooth.

In 12 groups of data obtained from 35-year-old, 46-year-old and 68-year-old, three out of four sets of dental specimens, there exist only two groups of the Young's modulus obtained by CSM and SLM, respectively, having the difference gap of 10 GPa. There exists little difference of the Young's moduli of enamel obtained by CSM or SLM, respectively, under normal circumstances. Compared to other three sets, 75-year -old tooth specimen displays bigger difference of tooth enamel between CSM and SLM measurements. Similar situation

occurs in the load-displacement relationship diagram. The speculated relevant factors are non-homogeneous tooth enamel material [15], directional of the tooth microstructure [16], dental caries under the measurement surface, etc. Overall, CSM measured Young's modulus show maximum value of 103.87GPa, minimum value of 74.04 GPa, the difference of 29.83 GPa. SLM measured Young's modulus show maximum value of 100.48 GPa, minimum value of 58.86 GPa, the difference of 41.62 GPa. There exists small difference between the CSM measurement data.

From Tables 1 to 4, four sets of tooth specimens cannot prove that the value of the Young's modulus is related to the age. Previous study presented the similar results [17-19]. The largest average of Young's modulus measured from both SLM and CSM is 68-year-old tooth specimen, followed by 35-year-old specimen. Possible causes are differences in the teeth, genetic, and eating habits [20]. The teeth are varied from different sources and are needed huge dental specimens of different ages to verify the existence of relationship between Young's modulus and age.

5. Conclusions

By using the nano-indentation measurement system and continuous stiffness measurement method, the results show the Young's moduli of the tooth enamel from 74GPa to 104GPa. Data show greater variation in shallower region of indentation depth, and the corresponding obtained Young's modulus may less suitable for dental material reference. The Young's modulus and its standard deviation tend to decrease with indentation depth increases. The data on the maps appears to be more focused on Gaussian distribution. As SLM at the maximum loading between 20 and 180 mN, Young's modulus does not stabilized. When it is at the higher loading of 120 or 180 mN, twin peaks may appear and lead the measured average of Young's modulus to be increased. By comparing these two methods, CSM shows more stable values and trend, and it may be more applicable to measure the mechanical properties of tooth. Both CSM and SLM values are similar for 35-year-old, 46-year-old, 68-year-old tooth specimen, but the standard deviation of CSM is lower. Young's modulus on the 75-year-old tooth specimen has significantly difference between CSM and SLM which has yet to explore the differences in the measurements. Young's modulus does not perform a downward trend in the four sets of increasing age teeth specimens.

The results show that, in CSM mode, when the indentation depth is above 400 nm, the average Young's modulus will decrease slightly with

increasing indentation depth, and its corresponding standard deviation tends to gradually reduced and stabilized. On the other hand, Young's modulus acquired by SLM has no fixed trend, at the highest loading of 20 mN to 60 mN, the standard deviation become smaller. When the indentation depth increases as the load increases, the standard deviation becomes bigger. Based on the above measurement results, it is found that the CSM can provide more stable Young's modulus and is suitable to measure the mechanical properties of teeth.

Corresponding author: Jao-Hwa Kuang, Ph.D.
E-mail : kuang@faculty.nsysu.edu.tw

References

1. M.A.R. Ladez, S.R. Fakour and M. Karbasi, "Evaluation of interleukin 8, 12 & 33 Serum level in Patients with Chronic Periodontitis, Aggressive Periodontitis and Healthy Subjects," Life Science Journal, 9(4), pp. 111-117, 2012.
2. L.A. Shinawi, "Partial Edentulism: a Five Year Survey on the Prevalence and Pattern of Tooth Loss in a sample of Patients Attending King Abdul Aziz University - Faculty of Dentistry," Life Science Journal, 9(4), pp. 2665-2671, 2012.
3. A. C. Fischer-Cripps, Nano indentation, Springer- Verlag, New York, 2002.
4. K.E. El-Kholey and H. El-Shenaway, "Role Of Diode Laser In Preservation Of The Marginal Bone Around Early Loaded Endosseous Implant," Life Science Journal, 9(3), pp. 940-943, 2012.
5. A. Fathi and A.A. Al-Sharabasy, "Threshold of Pain Perception to Intraoral Anesthetic Injections among Egyptian Children," Life Science Journal, 9(3), pp.1480-1483, 2012.
6. X. Li, and B. Bharat, "A Review of Nano-indentation Continuous Stiffness Measurement Technique and its Applications," Materials Characterization, Vol. 48, pp. 11-36., 2002.
7. J. Collin, G. Mauvoisin, O. Bartier , R.E. Abdi and P. Pilvin, "Experimental evaluation of the stress–strain curve by continuous indentation using different indenter shapes", Materials Science and Engineering, A 501, 140–145, 2009.
8. I. N. Sneddon, "The Relation between Load and Penetration in the Axisymmetric Boussinesq Problem for a Punch of Arbitrary Profile," International Journal of Engineering Science, Vol. 3, pp. 47-57, 1965.
9. W.C. Oliver, G.M. Pharr, "An Improved Technique for Determining Hardness and Elastic Modulus Using Load and Displacement Sensing Indentation Experiments," Journal of Materials Research, Vol. 7 No.6, pp.1564-1583, 1992.
10. J. B. Pethica, R. Hutchings and W.C. Oliver, "Hardness Measurement at Penetration as small as 20 nm," Philosophical Magazine A, Vol. 48, pp.593-606, 1983.
11. M. K. Shorshorov, S.I. Bulychev, and V. P. Alekhin, "Work of Plastic and Elastic Deformation During Indenter Indentation," Soviet Physics - Doklady, Vol. 26, pp. 769-771, 1981.
12. G.M. Pharr, W.C. Oliver, and F.R. Brotzen, "On the Generality of the Relationship among Contact Stiffness Contact Area, and Elastic Modulus during Indentation," Journal of Materials Research, Vol. 7, pp. 613-617, 1992.
13. N.A. Stillwell and D. Tabor, "Elastic Recover of Conical Indentations", Proc. Phys. Soc. London, Vol. 78, pp. 169-179, 1961.
14. J. Zhou, L.L. Hsiung, "Depth-dependent mechanical properties of enamel by nano-indentation", Journal of Biomedical Materials Research, Vol. 81A, pp. 67-74, 2006.
15. R.G. Craig, F.A. Peyton, "The Microhardness of enamel and dentin", Journal of Dental Research, vol.37 No.4, pp. 661-668, 1958.
16. H. Jiang, X.-Y. Liu, C.T. Lim, C.Y. Hsu, "Ordering of self-assembled nanobiominerals in correlation to mechanical properties of hard tissues," Appl. Phys. Lett., Vol. 86, pp. 163901-163903, 2005.
17. P.J. Chiu, H.L. Chien, H.K. Chen, J.-H. Kuang, " Investigate the Young's modulus of the teeth by using a different ratio of the nano-indentation unloading curve data," The 34th National Conference on Theoretical and Applied Mechanics, National Yunlin University of Science and Technology, November 19-20, 2010.
18. T.L. Wei, H.L. Chien, W.I. Zhan, J.-H. Kuang, "Nano-indentation tests for the Young's modulus of the teeth," The 35th National Conference on Theoretical and Applied Mechanics, National Cheng Kung University, November 18-19, 2011.
19. H.-L. Chien, P.-J. Chiu, B.W. Huang, J.-H. Kuang, "Young's Moduli of Human Tooth Measured using Micro-Indentation Tests," Life Science Journal, 9(2), pp. 172-177, 2012.
20. B.R.H. Nizam, C.T. Lim, H.K. Chang, A.U.J. Yap, "Nanoindentation study of human premolars subjected to bleaching agent," Journal of Biomechanics, Vol. 38, pp. 2204-2211, 2005.

3/14/2013